Structural Engineering and Mechanics, Vol. 8, No. 2 (1999) 207-231
DOI: http://dx.doi.org/10.12989/sem.1999.8.2.207

Defect-free 4-node flat shell element: NMS-4F element

Chang-Koon Choi† and Phill-Seung Lee‡

Department of Civil Engineering, Korea Advanced Institute of Science and Technology, Taejon 305-701, Korea

Yong-Myung Park‡†

Steel Str. Tech. Div., Research Institute of Industrial Science & Technology, Kyungkido 445-810, Korea

Abstract. A versatile 4-node shell element which is useful for the analysis of arbitrary shell structures is presented. The element is developed by flat shell approach, i.e., by combining a membrane element with a Mindlin plate element. The proposed element has six degrees of freedom per node and permits an easy connection to other types of finite elements. In the plate bending part, an improved Mindlin plate has been established by the combined use of the addition of non-conforming displacement modes (N) and the substitute shear strain fields (S). In the membrane part, the non-conforming displacement modes are also added to the displacement fields to improve the behavior of membrane element with drilling degrees of freedom and the modified numerical integration (M) is used to overcome the membrane locking problem. Thus the element is designated as NMS-4F. The rigid link correction technique is adopted to consider the effect of out-of-plane warping. The shell element proposed herein passes the patch tests, does not show any spurious mechanism and does not produce shear and membrane locking phenomena. It is shown that the element produces reliable solutions even for the distorted meshes through the analysis of benchmark problems.

Key words: shell element; non-conforming mode, plate element; membrane element; drilling degree of freedom; substitute shear strain; modified integration; rigid link correction.

1. Introduction

Shells have been used for many engineering structures due to the merits of their structural behaviors and the evolution of finite element technologies played important roles for advances of shell analysis and design. The problem of shell finite elements is still an open one because of the difficulty in satisfying the following conditions for an element, all of which should be satisfied so as to offer an efficient shell element: i) the adjustment for thick and thin cases, i.e., the requirements for no shear and membrane locking; ii) six degrees of freedom per node; iii) the fast

† Institute Chair Professor
‡ Graduate Student
‡† Senior Researcher

convergence characteristics; iv) insensitivity for mesh distortion (in-plane and out-of-plane); v) passing a patch test and correct rank, i.e., the requirements for no spurious zero-energy mode; and vi) the ease of formulation.

A great deal of research work has been devoted to develop shell elements which satisfy the above conditions through the following three major approaches: i) the degenerated shell elements derived from three-dimensional solid elements; ii) the flat shell element formulation; and iii) the curved shell elements based on classical shell theory. Among these approaches, the degenerated shell and flat shell elements have been more frequently used because of their generality in formulation and modeling. The degenerated shell element which was first proposed by Ahmad and Irons with the form of biquadratic element has five degrees of freedom per node and exhibits 'shear locking' and 'membrane locking' in the thin shell case (Ahmad *et al.* 1968). Despite its complicated formulation, a lot of researchers' efforts have been being devoted to develop a more efficient degenerated shell element and recently they have been expanded to an element with six degrees of freedom per node including the rotational degree of freedom (Kebari and Cassell 1991, Chroscielewski *et al.* 1997). On the other hand, the flat shell element was first developed by Gallagher (1974) with triangular element by combining the plate bending element with a membrane element. The major advantage of flat shell is a simplicity in its formulation but for some shell problems, too many flat shell elements are required to obtain a reasonably accurate solution. Thus, parallel to the research to develop more accurate flat shell elements, efforts to develop the modified flat shell element to be used for general shell problems are also in progress (Taylor 1987, Cook 1994, Groenwold and Stander 1995).

The main objective of this paper is to propose a defect-free 4-node non-conforming flat shell element, which has been developed basically by combining a membrane element with drilling degree of freedom and a Mindlin plate bending element (see Fig. 1). The element possesses six degrees of freedom per node which, in addition to improvement of the element behavior, permits an easy connection to other types of element with six degrees of freedom per node. The plate bending part of this shell element has been established by the combined use of the addition of non-conforming modes and the substitute shear strain fields. Non-conforming modes are added to the rotational degree of freedom to improve the flexural behavior in the distorted mesh in particular (Kim and Choi 1992, Choi *et al.* 1998). The membrane part is formulated by the modification of the membrane element of Ibrahimbegovic *et al.* (1990) which has the drilling degree of freedom. To remove the membrane locking shown in the shell element with the Ibrahimbegovic's displacement formulation of membrane element, Groenwold and Stander (1995) applied the modified 5-point reduced integration scheme to the original formulation and obtained more improved results. The same integration scheme, i.e., 5-point integration scheme, is applied to the Ibrahimbegovic's mixed formulation, to obtain a series of more improved elements in this study. Among the resulted membrane elements, the best performing element is selected to use in the development of shell element.

The formulation of a flat shell element is possible only when all of its nodes are on the planar plane from a definition of flat shell. Otherwise, it can not solve the shell problem with a warped geometry. The rigid link correction method of Taylor (1987) is adopted to overcome the out-of-plane warpage problems.

Over a past few decades, a lot of research efforts have been directed at overcoming the shear locking problems in the Mindlin plate elements, which are the major deficiency of the kind of element, thus rendering them more effective and reliable for the thin plate applications (Choi 1984, 1986, Hinton and Huang 1986, Hughes *et al.* 1978, 1981, Lee and Wong 1982, Parisch 1979,

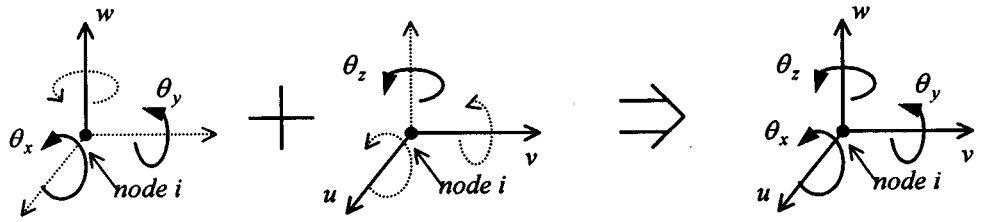

(DOF of plate) (DOF of membrane with Drilling DOF) (DOF of shell with six DOF)

Fig. 1 The six degrees of freedom per node

Zienkiewicz *et al.* 1971). As results of these research efforts, several successful remedial schemes have been suggested: namely, the reduced (or selective) integration technique (Zienkiewicz *et al.* 1971, Hughes *et al.* 1978); the addition of non-conforming displacement modes (Choi and Schnobrich 1975, Choi 1984); and the use of substitute shear strain fields (Hughes and Tezduyar. 1981, Hinton and Huang 1986, Donea and Lamain 1987). Efforts have been also devoted to the development of plate bending elements by the combined use of aforementioned schemes and quite successful results have been reported (Choi *et al.* 1984, 1986, and 1991, Kim and Choi 1992). Based on the evolution of the concept of combined use of non-conforming modes and other remedical schemes, the development of a new 4-node Mindlin plate finite element is one of the main concerns of this paper.

The shell element proposed in this study passes the patch tests, does not show any spurious mechanism, and does not produce shear and membrane locking phenomena. It is acknowledged from the analysis of the selected benchmark problems that the element produces reliable solutions even for distorted meshes.

2. Formulation of shell element

2.1. New improved 4-node Mindlin plate elements

The Mindlin plate elements have been successfully used in a wide range of plate analysis problems. The inter-element compatibility requirement in the plate elements is easily satisfied by this element because the shape functions require only C^0 continuity. However, this element has one significant deficiency, i.e., the excessive shear stiffness due to the transverse displacement constraint in a thin plate. The assumed displacement shape functions used in the isoparametric element constrain the element to deform in a shear mode imposing a large amount of the shearing strain in the bending behavior of a plate element, which causes a very slow convergence. In addition, since the ratio of shear stiffness coefficients to the bending stiffness coefficients of the element is the order of $(L/t)^2$, the shear stiffness becomes dominant in the element stiffness as the thickness of the plate t becomes thin. The performance of the Mindlin plate elements, therefore, deteriorates rapidly in the thin structures and these problems are known as the shear locking.

The development of an improved Mindlin plate element can be accomplished by the addition of non-conforming modes and by the substitute shear strain field. To improve the flexural behaviors, two non-conforming modes $\overline{N}_1$, $\overline{N}_2$ in Fig. 2 are added to the rotational displacement fields of isoparametric 4-node element. Then, the new displacement fields are expressed as follows:

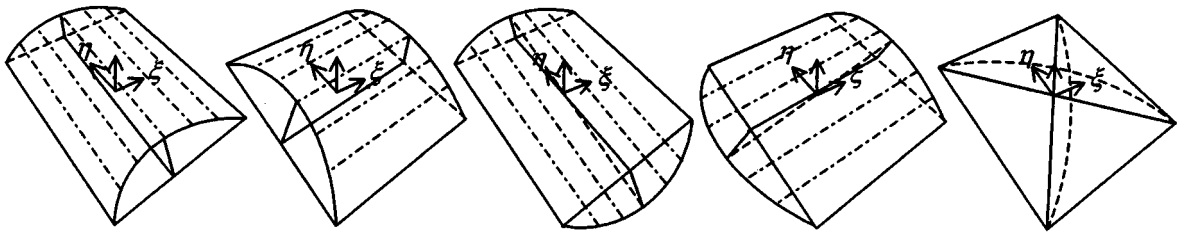

(a) $\bar{N}_1$ (b) $\bar{N}_2$ (c) $\bar{N}_3$ (d) $\bar{N}_4$ (e) $\bar{N}_5$

Fig. 2 The non-conforming modes for four-node elements

$$\begin{aligned} w &= <N>\{w\} \\ \theta_x &= <N>\{\theta_x\} + <\bar{N}>\{\bar{\theta}_x\} \\ \theta_y &= <N>\{\theta_y\} + <\bar{N}>\{\bar{\theta}_y\} \end{aligned} \tag{1}$$

in which $<N>$ is the matrix of the original 4-node isoparametric shape functions, Eq. (2), $<\bar{N}>$ is the matrix of the non-conforming modes in Eq. (3). $\{w\}$, $\{\theta_x\}$ and $\{\theta_y\}$ are the transverse displacements and two rotations about x and y axis (Fig. 1), respectively, and $\bar{\theta}_x$ and $\bar{\theta}_y$ are the non-conforming rotational displacements. The nonconforming modes used for bilinear elements are shown in Fig. 2.

$$N_1 = \frac{1}{4}(1-\xi)(1-\eta),\ N_2 = \frac{1}{4}(1+\xi)(1-\eta),\ N_3 = \frac{1}{4}(1+\xi)(1+\eta),\ N_4 = \frac{1}{4}(1-\xi)(1+\eta) \tag{2}$$

$$\bar{N}_1 = 1-\xi^2,\ \bar{N}_2 = 1-\eta^2,\ \bar{N}_3 = \eta(1-\xi^2),\ \bar{N}_4 = \xi(1-\eta^2),\ \bar{N}_5 = (1-\xi^2)(1-\eta^2) \tag{3}$$

Eq. (4) shows the displacement-strain relationship in which the submatrices associated with the addition of non-conforming modes are appended to the original isoparametric Mindlin plate element.

$$\begin{Bmatrix} \varepsilon_x \\ \varepsilon_y \\ \gamma_{xy} \\ \gamma_{yz} \\ \gamma_{xz} \end{Bmatrix} = \left[\begin{array}{ccc:cc} <0> & <0> & z\dfrac{\partial <N>}{\partial x} & <0> & z\dfrac{\partial <\bar{N}>}{\partial x} \\ <0> & -z\dfrac{\partial <N>}{\partial y} & <0> & -z\dfrac{\partial <\bar{N}>}{\partial y} & <0> \\ <0> & -z\dfrac{\partial <N>}{\partial x} & z\dfrac{\partial <N>}{\partial y} & -z\dfrac{\partial <\bar{N}>}{\partial x} & z\dfrac{\partial <\bar{N}>}{\partial y} \\ \hdashline \dfrac{\partial <N>}{\partial y} & <L^{\theta_x}> & <L^{\theta_y}> & -<\bar{N}> & <0> \\ \dfrac{\partial <N>}{\partial x} & <M^{\theta_x}> & <M^{\theta_y}> & <0> & <\bar{N}> \end{array}\right] \begin{Bmatrix} \{w\} \\ \{\theta_x\} \\ \{\theta_y\} \\ \{\bar{\theta}_x\} \\ \{\bar{\theta}_y\} \end{Bmatrix} \tag{4}$$

In Eq. (4), $<L^{\theta_x}>$, $<L^{\theta_y}>$, $<M^{\theta_x}>$ and $<M^{\theta_y}>$ are the modified shape functions for the substitute shear strain fields (Donea and Lamain 1987). The Eq. (4) can be rewritten in a condensed form.

$$\{\varepsilon\} = \begin{bmatrix} \boldsymbol{B}_b & \bar{\boldsymbol{B}}_b \\ \widetilde{\boldsymbol{B}}_s & \bar{\boldsymbol{B}}_s \end{bmatrix} \begin{Bmatrix} \boldsymbol{u} \\ \bar{\boldsymbol{u}} \end{Bmatrix} \tag{5}$$

where the submatrices $\bar{\boldsymbol{B}}_b$ and $\bar{\boldsymbol{B}}_s$ are the strain matrices associated with the non-conforming displacements and the submatrix $\widetilde{\boldsymbol{B}}_s$ is shear strain matrix by the substitute strain fields suggested by Donea and Lamain (1987). The subscript b and s indicate bending and shear, respectively.

In general, the non-conforming modes make a change of the strain energy (likely reduce the energy) in an element and give rise to the failure of patch test. Thus, to overcome this phenomenon the B-bar method (Zienkiewicz and Taylor 1989) is used in which the submatrices $\bar{\boldsymbol{B}}_s$ and $\bar{\boldsymbol{B}}_b$ are then substituted by $\bar{\boldsymbol{B}}_s{}^*$ and $\bar{\boldsymbol{B}}_b{}^*$ defined in Eqs. (6) and (7).

$$\bar{\boldsymbol{B}}_b{}^* = z\left(\frac{1}{z}\bar{\boldsymbol{B}}_b - \frac{1}{V}\int_V \frac{1}{z}\bar{\boldsymbol{B}}_b \, dV\right) \tag{6}$$

$$\bar{\boldsymbol{B}}_s{}^* = \bar{\boldsymbol{B}}_s - \frac{1}{V}\int_V \bar{\boldsymbol{B}}_s \, dV \tag{7}$$

The element stiffness matrix has been enlarged over the original isoparametric element matrix due to the addition of non-conforming displacement modes and related unknowns $\bar{u}$. Then the matrix is partitioned as follows:

$$\begin{bmatrix} \boldsymbol{K}_{cc} & \boldsymbol{K}_{cn} \\ \boldsymbol{K}_{cn}^T & \boldsymbol{K}_{nn} \end{bmatrix} \begin{Bmatrix} \boldsymbol{u} \\ \bar{\boldsymbol{u}} \end{Bmatrix} = \begin{Bmatrix} \boldsymbol{f} \\ \boldsymbol{0} \end{Bmatrix}, \quad \bar{\boldsymbol{u}} = -\boldsymbol{K}_{nn}^{-1}\boldsymbol{K}_{cn}^T \tag{8}$$

The enlarged stiffness matrix in Eq. (8) can be condensed back to the same size as the stiffness matrix of the ordinary Mindlin plate element (Choi and Schnobrich 1975)

$$\boldsymbol{K} = \boldsymbol{K}_{cc} - \boldsymbol{K}_{cn}\boldsymbol{K}_{nn}^{-1}\boldsymbol{K}_{cn}^T \tag{9}$$

where $\boldsymbol{K}_{cc}$, $\boldsymbol{K}_{cn}$ and $\boldsymbol{K}_{nn}$ are defined as,

$$\begin{aligned} \boldsymbol{K}_{cc} &= \int_V \boldsymbol{B}_b^T\boldsymbol{D}_b\boldsymbol{B}_b \, dV + \int_V \widetilde{\boldsymbol{B}}_s{}^T\boldsymbol{D}_s\widetilde{\boldsymbol{B}}_s \, dV \\ \boldsymbol{K}_{cn} &= \int_V \boldsymbol{B}_b^T\boldsymbol{D}_b\bar{\boldsymbol{B}}_b{}^* \, dV + \int_V \widetilde{\boldsymbol{B}}_s{}^T\boldsymbol{D}_s\bar{\boldsymbol{B}}_s{}^* \, dV \\ \boldsymbol{K}_{nn} &= \int_V \bar{\boldsymbol{B}}_b{}^{*T}\boldsymbol{D}_b\bar{\boldsymbol{B}}_b{}^* \, dV + \int_V \widetilde{\boldsymbol{B}}_s{}^{*T}\boldsymbol{D}_s\bar{\boldsymbol{B}}_s{}^* \, dV \end{aligned} \tag{10}$$

Eliminating the non-conforming displacements using Eq. (8), stresses can be computed by

$$\{\sigma\} = [D][\boldsymbol{B} \;\; \bar{\boldsymbol{B}}] \begin{Bmatrix} \boldsymbol{u} \\ \bar{\boldsymbol{u}} \end{Bmatrix} = [D][\boldsymbol{B} - \bar{\boldsymbol{B}}\,\boldsymbol{K}_{nn}^{-1}\boldsymbol{K}_{cn}^T]\,\{\boldsymbol{u}\} \tag{11}$$

where $\boldsymbol{B}$ and $\bar{\boldsymbol{B}}$ are $\begin{bmatrix} \boldsymbol{B}_b \\ \widetilde{\boldsymbol{B}}_s \end{bmatrix}$ and $\begin{bmatrix} \bar{\boldsymbol{B}}_b{}^* \\ \bar{\boldsymbol{B}}_s{}^* \end{bmatrix}$, respectively, and $[D]$ is the material rigidity matrix.

Based on the selection of the remedial schemes, a number of different versions of element formulation are possible from Eq. (9) and the elements in a series are systematically designated as

Table 1 The series of Mindlin plate elements

Designations	Displacement fields		Integration orders		Shear
	w	θ_x, θ_y	Bending	Shear	
NMS-4Pa (Donea and Lamain 1987)	$<N>\{w\}$	$<N>\{\theta\}$	2×2	2×2	Substitute
NMS-4Pb (this study)	$<N>\{w\}$	$<N>\{\theta\}+<\bar{N}>\{\bar{\theta}\}$	2×2	2×2	Substitute
NMS-4Pc (this study)	$<N>\{w\}$	$<N>\{\theta\}+<\bar{N}>\{\bar{\theta}\}$	2×2	1×1	Substitute

NMS-4Px which indicates "Nonconforming Modified integrated Shear substitute 4-node Plate element - version x". In this study, three different types of Mindlin plates in the series are considered (Table 1): i) the element designated as NMS-4Pa which is modified by substitute shear strain field only (Donea and Lamain 1987); ii) the element NMS-4Pb which is modified by addition of non-conforming modes to the Donea and Lamain formulation; iii) the element NMS-4Pc which is modified by reduced integration for the shear stiffness of the element. A comparison will be made on the elements to identify the best plate bending element for the use in the development of the defect-free shell element.

2.2. Membrane element with drilling degree of freedom

Generally membrane elements have two translational degrees of freedom (u, v) per node, but the need for the membrane element with a drilling degree of freedom, i.e., the rotation about the axis normal to the plane of element, arises in many practical engineering problems. When this element is combined with a plate bending element discussed in the previous section, a flat shell element can be constructed which has six degrees of freedom per node. This type of element is useful in solving a continuously curved surface or folded plate structures and provides a easy coupling with edge beams or rib members which have six degrees of freedom per node. Inclusion of a drilling degree of freedom (θ_z) gives also the improved behavior of the element (Allman 1984, Choi and Lee 1996).

The possibility of membrane elements with drilling degree of freedom was opened by Allman (1984), Bergan and Fellipa (1985). The concept has been further elaborated by many other researchers (Cook 1986, MacNeal and Harder 1988, Ibrahimbegovic *et al.* 1990, Choi and Lee 1996) for more improved elements. Ressiner (1965) first suggested a variational formulation that includes drilling degree of freedom as an independent rotation with the skew symmetric part of displacement gradient. Hughes and Brezzi (1989) extended Reissner's formulation to suggest a way in which the discrete approximation could be stabilized by using the independent rotation field based on the separate kinematic variables of displacement and rotation.

In this study, the Allman's (1984) rotational fields and a variational formulation suggested by Hughes and Brezzi (1989) are used as the basic schemes in order to construct membrane elements with drilling degree of freedom. To obtain the further improved elements, non-conforming modes are added to the translational and rotational degrees of freedom (Ibrahimbegovic *et al.* 1990) and this mixed type formulation is integrated by the modified 5-point integration rule in this study.

Thus, the displacement field of membrane element is constructed by the 4-node isoparametric shape functions $<N>$, rotational fields $<C>$ and $<S>$ and their non-conforming counterparts $<\bar{N}>$, $<\bar{C}>$ and $<\bar{S}>$, respectively.

$$u = <N>\{u\} + <C>\{\theta_z\} + <\bar{N}>\{\bar{u}\} + <\bar{C}>\{\bar{\theta}_z\}$$
$$v = <N>\{v\} + <S>\{\theta_z\} + <\bar{N}>\{\bar{v}\} + <\bar{S}>\{\bar{\theta}_z\}$$
$$\theta_z = <N>\{\theta_z\} \tag{12}$$

where $\{\bar{u}\}$, $\{\bar{v}\}$ and $\{\bar{\theta}_z\}$ are the non-conforming displacements. $<C>$ and $<S>$ are Allman's rotational fields of 4-node element. These are expressed as

$$C_j = \frac{1}{8}(c_{ij}l_{ij}P_{ij} - c_{jk}l_{jk}P_{jk}), \quad S_j = \frac{1}{8}(s_{ij}l_{ij}P_{ij} - s_{jk}l_{jk}P_{jk}) \tag{13}$$

in which the subscript i is in the sequence of 4,1,2,3, subscript j is 1,2,3,4, subscript k is in 2,3,4,1 and P_{ij} is as follows:

$$P_{12} = \frac{1}{2}(1-\xi^2)(1-\eta), \quad P_{23} = \frac{1}{2}(1+\xi)(1-\eta^2),$$
$$P_{34} = \frac{1}{2}(1-\xi^2)(1+\eta), \quad P_{41} = \frac{1}{2}(1-\xi)(1-\eta^2), \tag{14}$$

In Eq. (14), l_{ij} is the length of side $i-j$, c_{ij} and s_{ij} are the components of direction cosine of the normal vector n_{ij} to side $i-j$ (Fig. 3).

To improve the behavior of membrane element, the bubble mode ($\bar{N}_5$) in Eq. (3) is added to the translational degree of freedom. The non-conforming modes in Eq. (15), which can be explained by Timoshenko's beam theory, is added to the tangential direction of an element side with respect to the rotational degree of freedom

$$\bar{C}_j = \bar{c}_{ij}P_{ij}, \qquad \bar{S}_j = \bar{s}_{ij}P_{ij} \tag{15}$$

in which the value of subscript i and j are the same as the sequence in Eq. (13) and $\bar{c}_{ij}$ and $\bar{s}_{ij}$ are the components of direction cosine of the tangential vector t_{ij} of side $i-j$. (Fig. 3).

The variational Eq. (16) is constructed by the equilibrium equations, the symmetry conditions for stress, the definition of rotation in terms of the displacement gradient, and the constitutive equations (Hughes and Brezzi 1989)

$$\begin{aligned} 0 = D\ \Pi_\gamma(u, \psi, skew\,\sigma)\cdot(v, \omega, skew\,\tau) \\ = \int_\Omega (symm\ \nabla v)\cdot C\cdot(symm\,\nabla u)\,d\Omega + \int_\Omega skew\,\tau^T\cdot(skew\,\nabla u - \psi)\,d\Omega \\ + \int_\Omega (skew\ \nabla v^T - \bar{\omega}^T)\cdot skew\,\sigma\,d\Omega - \gamma^{-1}\int_\Omega skew\,\tau^T\cdot skew\,\sigma\,d\Omega - \int_\Omega v\cdot f\,d\Omega \end{aligned} \tag{16}$$

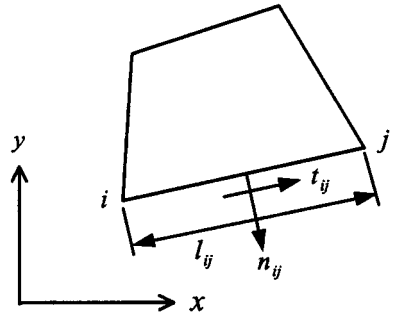

Fig. 3 The vector notations for a membrane element formulation

The symmetric part and skew-symmetric part of displacement are expressed by Eqs. (17) and (18) in the matrix form, respectively

$$symm\,\nabla u = [B]\begin{Bmatrix}\{u\}\\ \{v\}\end{Bmatrix} + [G]\{\theta_z\} + [\bar{B}]\begin{Bmatrix}\{\bar{u}\}\\ \{\bar{v}\}\end{Bmatrix} + [\bar{G}]\{\bar{\theta}_z\} \tag{17}$$

$$skew\,\nabla u - \theta_z = [b]\begin{Bmatrix}\{u\}\\ \{v\}\end{Bmatrix} + [g]\{\theta_z\} + [\bar{b}]\begin{Bmatrix}\{\bar{u}\}\\ \{\bar{v}\}\end{Bmatrix} + [\bar{g}]\{\bar{\theta}_z\} \tag{18}$$

where $[B]$, $[G]$, $[b]$ and $[g]$ are the conforming displacement-strain matrices, and $[\bar{B}]$, $[\bar{G}]$, $[\bar{b}]$ and $[\bar{g}]$ are the non-conforming displacement-strain matrices (Ibrahimbegovic *et al.* 1990).

Similar to the case of plate bending elements, the surplus strain energy due to the drilling degree of freedom and the non-conforming mode is removed by the B-bar method in order that the elements pass the patch tests. Thus matrices $\bar{\boldsymbol{B}}$, $\boldsymbol{G}$ and $\bar{\boldsymbol{G}}$ are modified as follows:

$$\bar{\boldsymbol{B}}^* = \bar{\boldsymbol{B}} - \frac{1}{V}\int_V \bar{\boldsymbol{B}}\,dV,\quad \boldsymbol{G}^* = \boldsymbol{G} - \frac{1}{V}\int_V \boldsymbol{G}dV,\quad \bar{\boldsymbol{G}}^* = \bar{\boldsymbol{G}} - \frac{1}{V}\int_V \bar{\boldsymbol{G}}\,dV \tag{19}$$

Particularly the B-bar method applied to $\boldsymbol{G}$ and $\bar{\boldsymbol{G}}$ is useful for mitigating the membrane locking caused by drilling degree of freedom (Taylor 1987). From Eqs. (16)~(18), Eq. (20) is constructed in a form of mixed formulation

$$\begin{bmatrix}\bar{\boldsymbol{K}} & \boldsymbol{h}^T\\ \boldsymbol{h} & -\gamma^{-1}V\end{bmatrix}\begin{Bmatrix}\boldsymbol{u}\\ \tau_0\end{Bmatrix} = \begin{Bmatrix}\boldsymbol{f}\\ 0\end{Bmatrix} \tag{20}$$

$$\boldsymbol{u} = \{\{u\}\ \{v\}\ \{\theta_z\}\ \{\bar{u}\}\ \{\bar{v}\}\ \{\bar{\theta}_z\}\}^T \tag{20a}$$

$$\boldsymbol{f} = \{\{f_u\}\ \{f_v\}\ \{f_{\theta_z}\}\ 0\ 0\ 0\}^T \tag{20b}$$

where

$$\bar{\boldsymbol{K}} = \begin{bmatrix}\bar{\boldsymbol{K}}_{cc} & \bar{\boldsymbol{K}}_{cn}\\ \bar{\boldsymbol{K}}_{cn}^T & \bar{\boldsymbol{K}}_{nn}\end{bmatrix} \tag{21}$$

$$\bar{\boldsymbol{K}}_{cc} = \int_V [\boldsymbol{B}\ \boldsymbol{G}^*]^T\,\boldsymbol{D}\,[\boldsymbol{B}\ \boldsymbol{G}^*]\,dV \tag{21a}$$

$$\bar{\boldsymbol{K}}_{cn} = \int_V [\boldsymbol{B}\ \boldsymbol{G}^*]^T\,\boldsymbol{D}\,[\bar{\boldsymbol{B}}^*\ \bar{\boldsymbol{G}}^*]\,dV \tag{21b}$$

$$\bar{\boldsymbol{K}}_{nn} = \int_V [\bar{\boldsymbol{B}}^*\ \bar{\boldsymbol{G}}^*]^T\,\boldsymbol{D}\,[\bar{\boldsymbol{B}}^*\ \bar{\boldsymbol{G}}^*]\,dV \tag{21c}$$

$$\boldsymbol{h} = \int_V [\boldsymbol{b}\ \boldsymbol{g}\ \bar{\boldsymbol{b}}\ \bar{\boldsymbol{g}}]^T\,dV \tag{22}$$

and

$$\gamma = \frac{E}{2(1+\nu)} \tag{23}$$

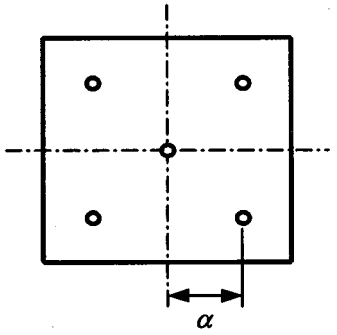

Fig. 4 The 5-point integration scheme

In Eq. (20), the constant τ_0 is skew-symmetric part of stress, and the parameter γ is a problem dependent constant (Hughes and Brezzi 1989). For the isotropic elasticity and Dirichlet boundary value problem, γ can be taken to be equal to the shear modulus as seen in Eq. (23).

The numerical integration rule used to calculate the submatrices of $\boldsymbol{K}$ in Eqs. (21a~c) and $\boldsymbol{h}$ in Eq. (22) is the 5-point integration scheme (Groenwold and Stander 1995). This integration technique is very useful to avoid membrane locking problems and the effectiveness will be shown in the hemishperical shell example (Fig. 17) later in this paper.

This integration scheme is defined as follows:

$$I^*(F) = W_0 F(0, 0) + W_\alpha F(\pm \alpha, \pm \alpha) \tag{24}$$

where $I^*(F)$ indicates the numerical approximation to the exact integral of the function F, and W_i indicates a weighting factor. In this study, W_0=0.01 is used

$$W_\alpha = 1 - W_0/4, \quad \alpha = \left(\frac{1}{3W_\alpha} \right)^{1/2} \tag{25}$$

Finally, the stiffness matrix of membrane element can be reduced to the dimension of conforming element by the static condensation of non-conforming displacements $\{\bar{u}\}$, $\{\bar{v}\}$ and $\{\bar{\theta}_z\}$, and stress term τ_0 in Eq. (20). The stresses of membrane element with drilling degree of freedom can be calculated as

$$\{\sigma\} = [D]\,[\boldsymbol{B} \;\; \boldsymbol{G}^*] \begin{Bmatrix} u \\ v \\ \theta_z \end{Bmatrix} \tag{26}$$

The same element designation system as that of plate elements is used except that P is replaced by M which stands for Membrane. Thus, the series of membrane elements which have different displacement fields are systematically designated as NMS-4Mo, NMS-4Ma, NMS-4Mb, and NMS-4Mc and listed in Table 2. NMS-4Mo is the original isoparametric element, NMS-4Ma has the rotational degree of freedom, NMS-4Mb is added with non-conforming mode to translational displacement and finally NMS-4Mc is added with non-conforming modes to both the translational and rotational degrees of freedom. A comparison will be made on those elements to choose the best membrane element with drilling degree of freedom for the development of a flat shell element.

Table 2 The series of membrane elements

Designations	Displacement fields			Integration orders
	u	v	θ_z	
NMS-4Mo (original isoparametric)	$\langle N\rangle \{u\}$	$\langle N\rangle \{v\}$	-	2×2
NMS-4Ma (This study)	$\langle N\rangle \{u\}+\langle C\rangle \{\theta_z\}$	$\langle N\rangle \{v\}+\langle S\rangle \{\theta_z\}$	$\langle N\rangle \{\theta_z\}$	5-point
NMS-4Mb (This study)	$\langle N\rangle \{u\}+\langle C\rangle \{\theta_z\}$ $+\langle \bar{N}\rangle \{\bar{u}\}$	$\langle N\rangle \{v\}+\langle S\rangle \{\theta_z\}$ $+\langle \bar{N}\rangle \{\bar{v}\}$	$\langle N\rangle \{\theta_z\}$	5-point
NMS-4Mc (This study)	$\langle N\rangle \{u\}+\langle C\rangle \{\theta_z\}$ $+\langle \bar{N}\rangle \{\bar{u}\}+\langle \bar{C}\rangle \{\bar{\theta}_z\}$	$\langle N\rangle \{v\}+\langle S\rangle \{\theta_z\}$ $+\langle \bar{N}\rangle \{\bar{v}\}+\langle \bar{S}\rangle \{\bar{\theta}_z\}$	$\langle N\rangle \{\theta_z\}$	5-point

2.3. Construction of shell element

When the nodes of flat shell elements are all in the same plane, the behavior of plate elements and that of membrane elements are uncoupled. Thus the stiffness matrix of a shell element can be formed by combining the plate stiffness and membrane stiffness obtained independently as follows;

$$[K]_{flat\ shell} = \begin{bmatrix} K_{plate} & 0 \\ 0 & K_{membrane} \end{bmatrix} \tag{27}$$

To solve the geometrically warped shell problems a flat shell element needs to be modified because its formulation is based on the flat geometry and uncoupled membrane and plate bending characteristics of the element. In order to take into account of the warped geometry, the rigid link correction is used (Taylor 1987). For the rigid link correction, the mean plane is formed by central point of each side and the distances between the mean plane and each nodes are taken to be the same ($|z_i|=h$). Then, the stiffness matrix is constructed at a mean plane which is the projection of warped geometry as shown in Fig. 5.

As seen in Fig. 5, the relationships for the kinematic conditions at nodes are

$$\theta_x' = \theta_x + z\cdot v, \quad \theta_y' = \theta_y - z\cdot u \tag{28}$$

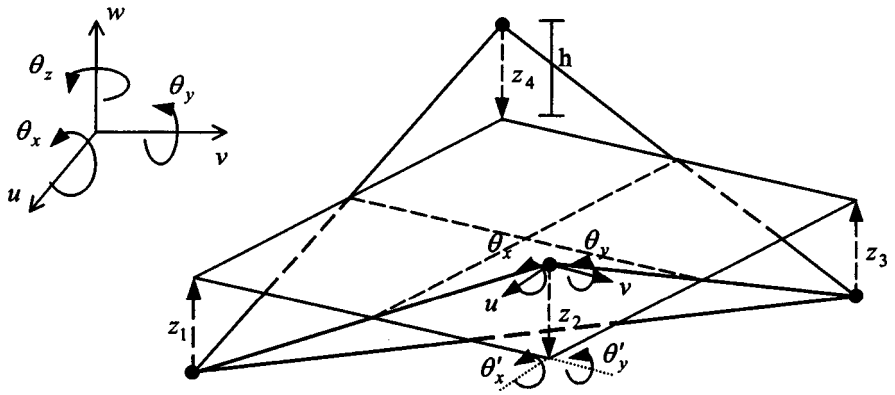

Fig. 5 The projection of warped geometry

The matrix form for each node is

$$\begin{Bmatrix} u' \\ v' \\ w' \\ \theta_x' \\ \theta_y' \\ \theta_z' \end{Bmatrix} = \begin{bmatrix} 1 & 0 & 0 & 0 & 0 & 0 \\ 0 & 1 & 0 & 0 & 0 & 0 \\ 0 & 0 & 1 & 0 & 0 & 0 \\ 0 & z & 0 & 1 & 0 & 0 \\ -z & 0 & 0 & 0 & 1 & 0 \\ 0 & 0 & 0 & 0 & 0 & 1 \end{bmatrix} \begin{Bmatrix} u \\ v \\ w \\ \theta_x \\ \theta_y \\ \theta_z \end{Bmatrix} \tag{29}$$

and when assembled for all the nodes in an element

$$\{\boldsymbol{u}'\} = [W]\{\boldsymbol{u}\} \tag{30}$$

where z defines the warpage at each node (which is constant and either h or $-h$ at each node) and quantities with a superscript act on the projection plane. The stiffness matrix considering the warpage effects is obtained with the rigid link correction matrix $[W]$ assembled as follows:

$$[K]_{local} = [W][K]_{flat}[W]^T \tag{31}$$

And then the element stiffness in the global coordinates system $[K]_{global}$ can be obtained by multiplying the rotation matrix $[R]$

$$[K]_{global} = [r]^T[K]_{local}[R] \tag{32}$$

This simple method to handle the warped geometry is very effective and produces a good result. It will be shown by the pre-twisted beam example (Fig. 18).

3. Numerical Test 1

3.1. Basic test

3.1.1. Eigenvalue test (Test #B1)

The eigenvalue analyses of the elements have been performed in order to check the presence of spurious zero energy modes with respect to both the Mindlin plate elements and the membrane elements. While the plate element NMS-4Pa and NMS-4Pb do not have any zero energy mode, the element NMS-4Pc has one. And all the membrane elements, i.e., NMS-4Ma, NMS-4Mb, and NMS-4Mc, do not exhibit any spurious mechanism.

3.1.2. Patch test (Test #B2)

The patch test is a simple numerical test widely accepted as a tool to verify the consistency and convergence of a finite element. For the proper test, a patch of distorted elements as shown in Fig. 6 is frequently used. Using the patch model, the consistent nodal loads that correspond to a state of constant strain are applied to the boundary nodes to describe pure strain states, i.e., the pure bending, the pure transverse shearing, and the pure twisting in the plate elements, and the pure tensioning and in-plane shearing in the membrane elements. In Table 3, it is shown that the plate element NMS-4Pc is the only element tested which does not pass the patch test due to rank deficiency.

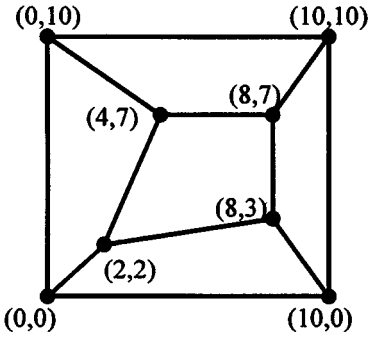

Fig. 6 Patch test model

Table 3 The patch test results

Elements	Plate Bending			Elements	In-plane	
	Bending	Shearing	Twisting		Tension	Shear
NMS-4Pa	Pass	Pass	Pass	NMS-4Mo	Pass	Pass
NMS-4Pb	Pass	Pass	Pass	NMS-4Ma	Pass	Pass
NMS-4Pc	Fail	Pass	Fail	NMS-4Mb	Pass	Pass
				NMS-4Mc	Pass	Pass

3.2. Test of plate element

3.2.1. Shear locking test (Test #P1)

To check the proposed Mindlin plate elements in a wide range of thickness-span ratios, the shear locking tests with an irregular mesh shape have been carried out. The selected mesh shape for the test is shown in Fig. 10b (the clamped square plate under central concentrated load). The test results for shear locking are shown in Fig. 7. Element NMS-4Pa and NMS-4Pb show a good result but the behavior of element NMS-4Pc is shown to be unreasonable. The result of element NMS-4Pb shows the best results in all the range of thickness-span ratios without showing any locking phenomenon.

3.2.2. Convergence test (Test #P2)

To examine convergence characteristics of the plate elements, a simply supported square plate under a uniform load is analyzed (Table 4 and Fig. 9). The theoretical value of deflection at the center is 4.062. The element NMS-4Pb shows the fastest convergence.

3.2.3. Square plate (Test #P3)

The 1/4 model of the clamped square plate under a uniform or a concentrated load as shown in Fig. 10 is tested with respect to the normal and distorted mesh.

The theoretical maximum displacement is 1.26 for the case of distributed load and 5.60 for the central concentrated load. The test results are shown in Table 4. The element NMS-4Pb exhibits better results than other elements.

3.2.4. Circular plate (Test #P4)

To check the robustness of the proposed Mindlin plate elements, a clamped circular plate under

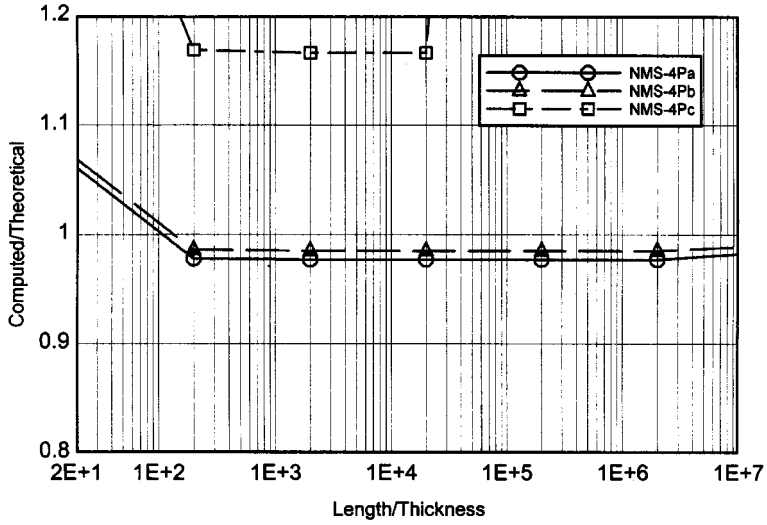

Fig. 7 The shear locking test

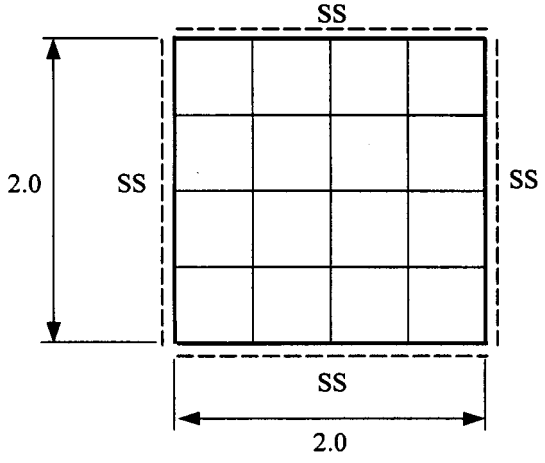

Young's Modulus = 17472000
Poisson's Ratio = 0.3
Thickness = 0.0001
Distributed Load =0.0001

Fig. 8 The model for convergence test

Table 4 The central deflection for simply supported square plate under a uniform load

Mesh	Elements		
	NMS-4Pa	NMS-4Pb	NMS-4Pc
2×2	3.189 (78.5%)	3.392 (83.5%)	8.893 (218.9%)
4×4	3.969 (97.7%)	4.018 (98.9%)	4.679 (115.2%)
8×8	4.041 (99.5%)	4.053 (99.8%)	4.329 (106.6%)
16×16	4.057 (99.9%)	4.062 (100%)	4.186 (103.1%)
Theory		4.062	

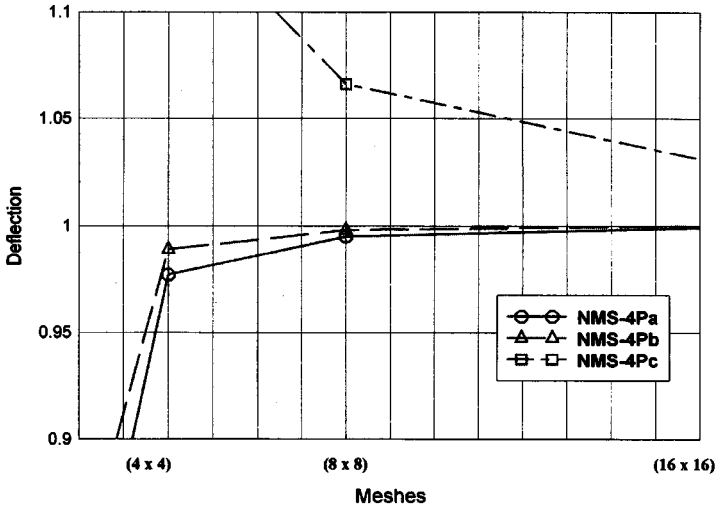

Fig. 9 Convergence test

the distributed load is analyzed. A quarter model considering symmetric condition is used. The theoretical value of the maximum bending moment is 8.125×10^{-2} at center. The test results are shown in Table 6.

3.2.5. Razzaque's 60° skew plate (Test #P5)

A 60° skew plate which is simply supported on two opposite edges and free on the other two edges and applied with a uniformly distributed load. Razzaque suggested 7.945×10^{5} for central deflection. The test results with refined meshes from this study are shown in Table 7.

3.3. Test of membrane element

3.3.1. Simple beam (higher order patch test - Test #M1)

A simple beam with a length to height ratio of 10 is subjected to a state of pure bending. The

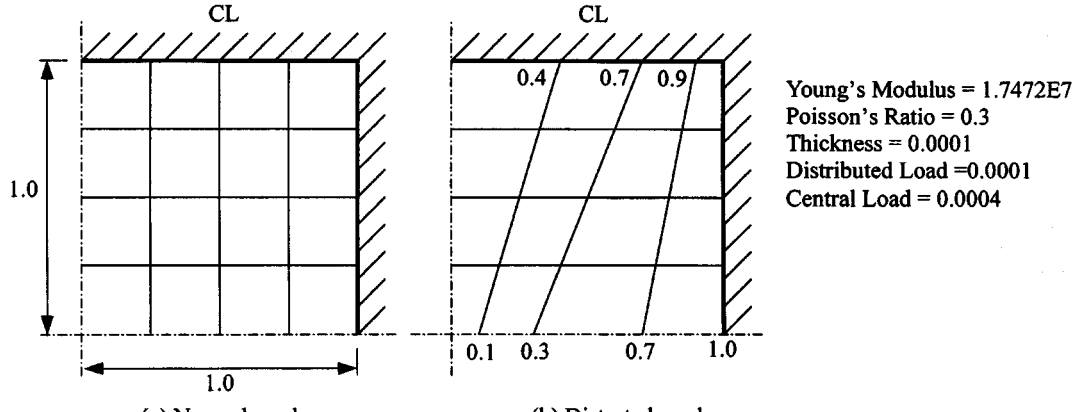

Fig. 10 The rectangular plate

Table 5 The maximum displacement of square plates

Loads	Meshes	Elements			
		NMS-4Pa	NMS-4Pb	NMS-4Pc	SAP (C&S inc.)
Distributed Load	Normal	1.251	1.257	1.330	1.319
	Distorted	1.278	1.286	1.374	1.355
Theory			1.26		
Concentrated Load	Normal	5.404	5.444	6.425	5.897
	Distorted	5.471	5.515	6.529	5.813
Theory			5.60		

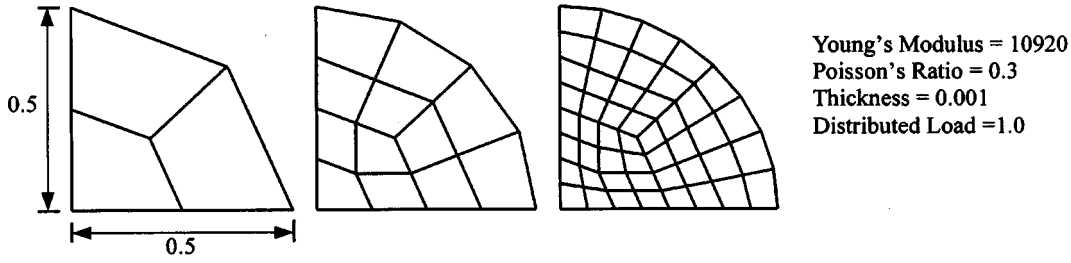

Fig. 11 Mesh of circular plate (N: number of elements)

beam is modeled with six membrane elements as shown in Fig. 13. Two load cases are considered; the first load case (Case I) is a unit couple (P=1.0) applied at the free ends and the second load case (CaseII) is a unit moment applied at the end nodes. The theoretical value obtained by beam theory is 1.5 for vertical displacement and 0.6 for end rotation.

The test results are shown in table 8 and it is acknowledged that except element NMS-4Mc which produces non-symmetric end rotations at both load cases, all the elements produced reliable results. It is noted that elements which have additional nonconforming modes (NMS-4Ma, NMS-4Mb, and NMS-4Mc) show more flexible results.

3.3.2. Cantilever beam (Test #M2)

A cantilever beam under shearing load as shown in Fig. 14 is selected as the next test problem. The theoretical elastic solution for the tip displacement is 0.3558. The test results are shown in Table 9.

Table 6 The maximum bending moment of circular plate ($\times 10^{-2}$)

No. of Elements	Elements			
	NMS-4Pa	NMS-4Pb	NMS-4Pc	Hinton and Huang (1986)
3	7.530	7.707	8.050	7.408
12	7.988	8.124	8.186	7.842
48	8.179	8.164	8.195	8.062
Theory			8.125	

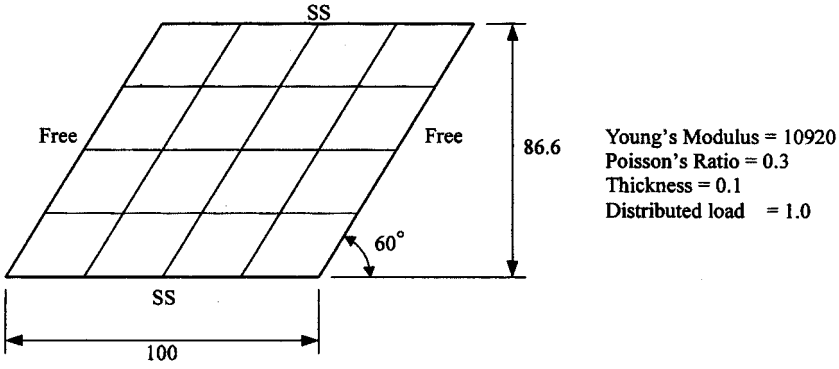

Fig. 12 Skew plate

Table 7 The central deflection of skew plate ($\times 10^5$)

Mesh	Elements			
	NMS-4Pa	NMS-4Pb	NMS-4Pc	SAP (C&S inc.)
4×4	6.722	6.764	7.465	7.736
8×8	7.591	7.615	7.907	7.870
16×16	7.826	7.834	7.953	-
Reference value		7.945		

3.3.3. Cook 's tapered panel under shear load (Test #M3)

This panel was proposed by Cook as a test for the accuracy of quadrilateral elements. Besides the shear dominated behavior, it also displays the effects of mesh distortion. The result for the tip deflection is compared with the reference value of 23.91 obtained by numerical analysis for a refined model.

3.4. Defect-free Flat Shell Element

Numerical test results are summarized in Table 11 in which the plate bending elements and the membrane elements are separately listed and each element is compared with the elements in the same group to identify the best performing element in each group. As seen in the Table, the element NMS-4Pb gave the best result for the plate bending problems and NMS-4Mb gave the best result for membrane problems. The competing plate element NMS-4Pc has a spurious mode

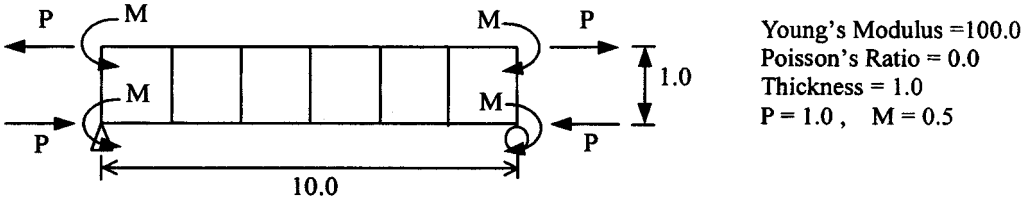

Fig. 13 Simple beam

Table 8 The higher order patch test

Elements	Case I		Case II	
	Vertical displacement	End rotation	Vertical displacement	End rotation
NMS-4Mo	1.5	-	1.5	-
NMS-4Ma	1.5	0.6	1.5102	0.64647
NMS-4Mb	1.5	0.6	1.5103	0.65046
NMS-4Mc	1.5	*	1.5200	*
Taylor and Simo (1985)	1.5	1.2	1.5	2.18980
Iura and Atluri (1992)	1.5	0.6	N/A	N/A
Ibrahimbegovic *et al.* (1990)	1.5	0.6	1.5	0.62070
Beam Theory	1.5	0.6	1.5	0.6

*non-symmetric rotations at both ends

and did not pass the patch test. And the competing membrane element NMS-4Mc shows the best behavior for the cantilever beam and the Cook's problem but makes unreasonable solutions for the higher order patch test. Thus, the linear combination of these two elements (Eq. (27)), designated as NMS-4Pb and NMS-4Mb, a highly effective new four-node flat shell element can be established. The new element has been designated as "NMS-4F" which indicate "Non-conforming Modified integrated Shear substitute 4-node Flat shell element". The behavior of this new element is tested in the following section.

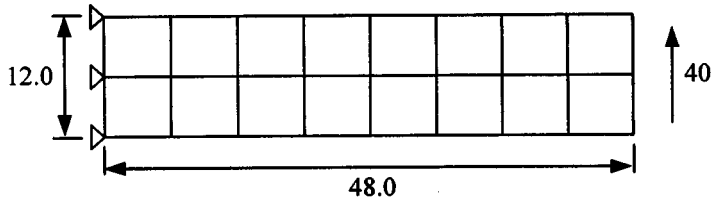

Fig. 14 Cantilever beam

Table 9 The tip displacements of cantilever beam

Elements	Meshes			
	1×4	2×8	4×16	8×32
NMS-4Mo	0.2424	0.3161	0.3446	0.3528
NMS-4Ma	0.3283	0.3460	0.3528	0.3550
NMS-4Mb	0.3445	0.3502	0.3539	0.3553
NMS-4Mc	0.3493	0.3516	0.3544	0.3554
Ibrahimbegovic *et al.* (1990)	0.3449	0.3525	0.3546	N/A
Frey (1989)	0.3283	0.3460	0.3529	N/A
Sabir (1985)	0.3281	0.3454	0.3527	N/A
Allman (1988)	0.3026	0.3394	0.3512	N/A
Theory	0.3558			

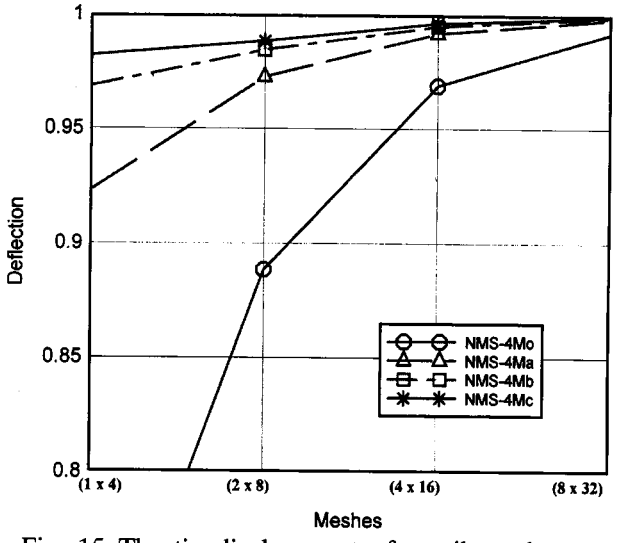

Fig. 15 The tip displacement of cantilever beam

4. Numerical Test II

4.1. Hemispherical shell with 18° hole

This is a problem in the set proposed by MacNeal and Harder (1985). This doubly curved shell problem is characterized by inextensible bending modes and large rigid body rotations. Thus the element with a membrane locking problem can not solve this example correctly. MacNeal and Harder suggests a value of 0.094 as a correct solution for the comparison of results for the displacement in the direction of applied load, and the more recent analyses suggest 0.093. Therefore, the exact value should be somewhere between these two values.

To show the effect of numerical integration scheme, both results by the 5-point integration scheme and the normal 3×3 gauss quardrature with present element are presented for the

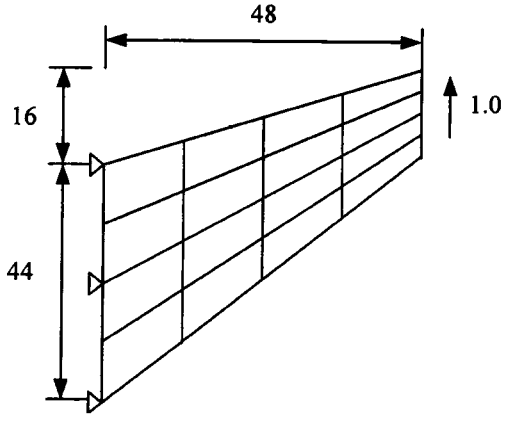

Young's Modulus = 1.0
Poisson's Ratio = 1/3
Thickness = 1.0

Fig. 16 Tapered panel

Table 10 The tip displacements of tapered panel

Elements	Meshes		
	2×2	4×4	8×8
NMS-4Mo	11.85	18.32	22.08
NMS-4Ma	20.14	22.56	23.55
NMS-4Mb	20.33	22.88	23.65
NMS-4Mc	21.52	22.96	23.69
Frey (1989)	20.09	22.61	23.55
Allman (1988)	20.27	22.78	23.56
Simo *et al.* (1989)	21.12	23.02	23.68
Cook (1986)	21.46	23.15	N/A
Reference		23.91	

Table 11 Summary of numerical test results of plates and membranes

Plate Elements				Membrane Elements			
Tests	NMS-4Pa	NMS-4Pb	NMS-4Pc	Tests	NMS-4Ma	NMS-4Mb	NMS-4Mc
Test #B1	○	○	×	Test #B1	○	○	○
Test #B2	○	○	×	Test #B2	○	○	○
Test #P1	**	***	×	Test #M1	***	***	×
Test #P2	**	***	*	Test #M2	*	**	***
Test #P3	**	***	*	Test #M3	*	**	***
Test #P4	*	**	***				
Test #P5	*	***	***				
The best element		○		The best element		○	

○: Pass, ×: Fail, ***: very good, **: good, *:poor

membrane part. It is recognized that the 5-point integration scheme is very effective for the elimination of membrane locking (Table 12).

4.2. Thick and thin pre-twisted beams

A pre-twisted beam example shown in Fig. 18 is tested in order to evaluate the behavior of the new flat shell element for warped geometry. Two different thicknesses are considered, namely t= 0.32(thick) and t=0.05(thin). The thick beam is a standard problem in the set proposed by MacNeal and Harder (1985), while the thin beam is taken from Jetteur (1986). The thin beam is tested to evaluate the locking phenomena. The pre-twisted geometry of this problem implies out-of-plane warp for quadrilateral shell elements. For the thick beam the analytical solutions are 5.424×10^{-3} and 1.754×10^{-3} for the displacements in direction of the in-plane force and the out-of-plane force, respectively. For the thin beam solutions obtained by Jetteur with isoparametric solid elements are used for comparison, which are 1.3857 and 0.3427 for in-plane and out-of-plane force, respectively.

The test results of the present element with rigid link correction are presented in Table 13 and 14.

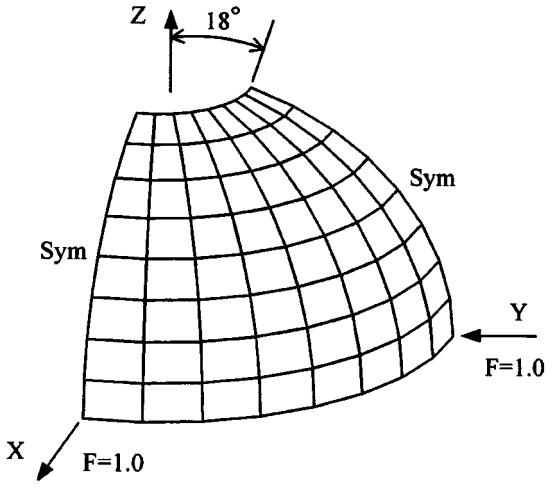

Fig. 17 Hemishperical shell

4.3. Scordelis-Lo roof

This is a problem in the set proposed by MacNeal and Harder (1985). The Scordelis-Lo roof is the singly curved shell problem in the proposed standard problem set. The theoretical value for the vertical displacement at the midpoint of the free edge is 0.3086, but most elements converge to a slightly lower value 0.3024. The results obtained are compared with some of the results available in the literature.

4.4. Curved box girder

A curved box girder shown in Fig. 20 is analyzed in order to investigate the usefulness of the proposed element for the analysis of the folded plate structure. The entire structural elements including flanges, curved webs, and diaphragms at supports are modeled by 444 elements. The dimensions of model and material characteristics are shown in Fig. 21. The solutions computed by the present element are compared with the experimental results reported by Fam and Turkstra (1976). The displacements shown in Fig. 22 exhibits good behaviors of this element.

Table 12 The displacement in direction of load

Meshes	Elements					
	NMS-4F (5-point)	NMS-4F (3×3)	SAP (C&S inc.)	Taylor (1987)	QC5D-SA (Groenwold and Stander 1995)	Simo *et al.* (1989)
2×2	0.03026	0.00726	0.02721	N/A	N/A	N/A
4×4	0.08793	0.01137	0.08753	0.08652	0.03631	0.09337
8×8	0.09297	0.05967	0.09372	0.09415	0.08935	0.09281
16×16	0.09315	0.08994	0.09349	0.09350	0.09312	0.09291
Reference	0.093-0.094					

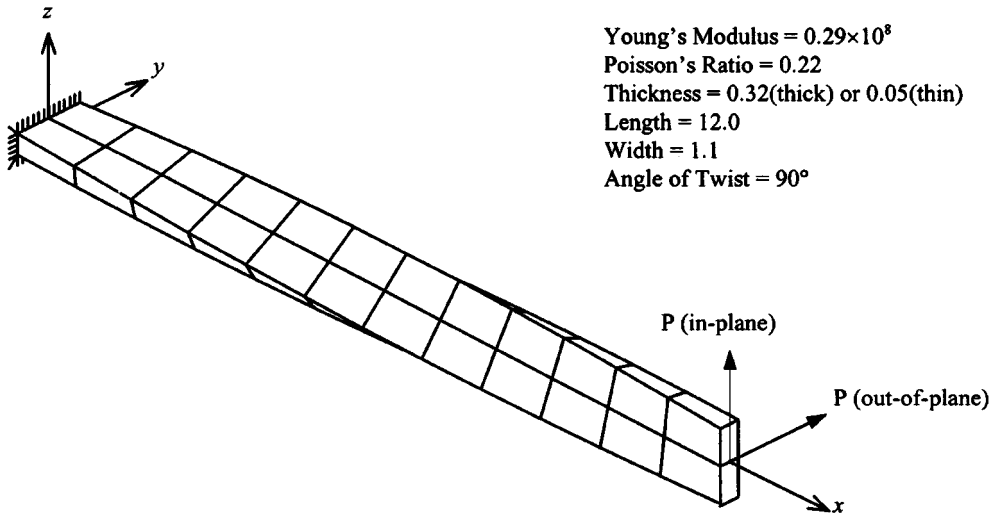

Fig. 18 Twisted beam

5. Conclusions

In this study, the development of a defect-free 4-node flat shell element with the drilling degree of freedom (designated as NMS-4F) has been presented. The element is established basically by the linear combination of the Mindlin plate element and the membrane element with drilling degrees of freedom. To improve the basic behavior of the element, several combinations of the improvement methods, i.e., the addition of non-conforming modes, the modified integration and the construction of assumed shear strain fields, have been performed independently in the formulation of element stiffness of plate and membrane part. For the improvement of Mindlin plate behavior, the quadratic nonconforming displacement modes (N) are added to the rotational degrees of freedom in addition to the use of the substitute shear strain fields (S). Similarly, in the membrane element with drilling degrees of freedom, nonconforming modes are added to the translations and tangential components of the drilling degree of freedom, and the modified numerical integration (M) is adopted to overcome membrane locking. From the results of standard

Table 13 The displacements in direction of load for thick beam ($\times 10^{-3}$)

Loads	Meshes	Elements			
		NMS-4F	SAP (C&S inc.)	Taylor (1987)	Frey (1989)
In-plane	1×6	5.391	5.408	5.402	5.335
	2×12	5.407	5.413	5.410	5.385
	4×24	5.413	5.405	5.403	5.397
Analytical value		5.424			
Out-of-plane	1×6	1.762	1.783	1.763	1.719
	2×12	1.758	1.770	1.763	1.742
	4×24	1.754	1.754	1.751	1.747
Analytical value		1.754			

Table 14 The displacements in direction of load for thin beam ($\times 10^{-3}$)

Loads	Meshes	Elements			
		NMS-4F	SAP (C&S inc.)	Taylor (1987)	Frey (1989)
In-plane	1×6	1.384	1.388	1.388	1.383
	2×12	1.385	1.389	1.389	1.384
	4×24	1.386	1.388	1.388	1.386
Reference value		1.3857			
Out-of-plane	1×6	0.3443	0.3503	0.3502	0.3443
	2×12	0.3434	0.3467	0.3466	0.3432
	4×24	0.3430	0.3435	0.3435	0.3429
Reference value		0.3427			

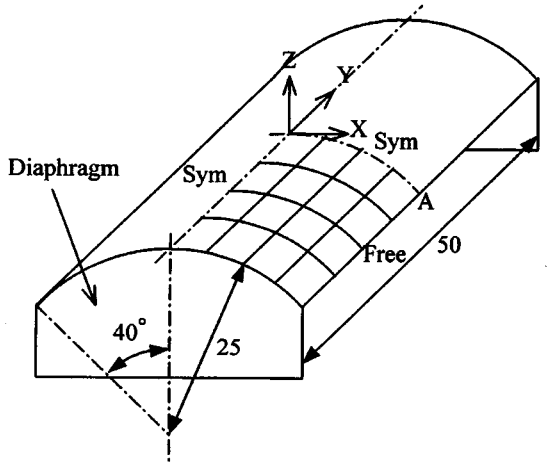

Young's Modulus = 4.32×10^8
Poisson's Ratio = 0.0
Thickness = 0.25
Gravity Load = 90 (uniform on surface area)

Fig. 19 Scordelis-Lo roof

benchmark analyses it has been found that the proposed flat shell element (NMS-4F) is highly efficient and robust. The element can be effectively used for not only the plate bending problems but also most shell problems with a reasonably refined mesh. The element is also defect-free, i.e., the element produces no shear and membrane locking, no spurious zero energy modes, and converges to the exact solutions fast even for the distorted meshes. This is the first work in NMS-

Table 15 The deflections at the midpoint of the free edge (point A)

Meshes	Elements				
	NMS-4F (This study)	SAP (C&S inc.)	Ibrahimbegovic and Frey (1994)	Taylor (1987)	Choi and Paik (1994)
2×2	0.4190	0.4207	0.4190	0.4207	N/A
4×4	0.3165	0.3169	0.3166	0.3169	0.3157
8×8	0.3039	0.3038	0.3039	0.3039	0.3030
16×16	0.3016	0.3013	0.3016	N/A	0.3009
Theory	0.3086 (0.3024)				

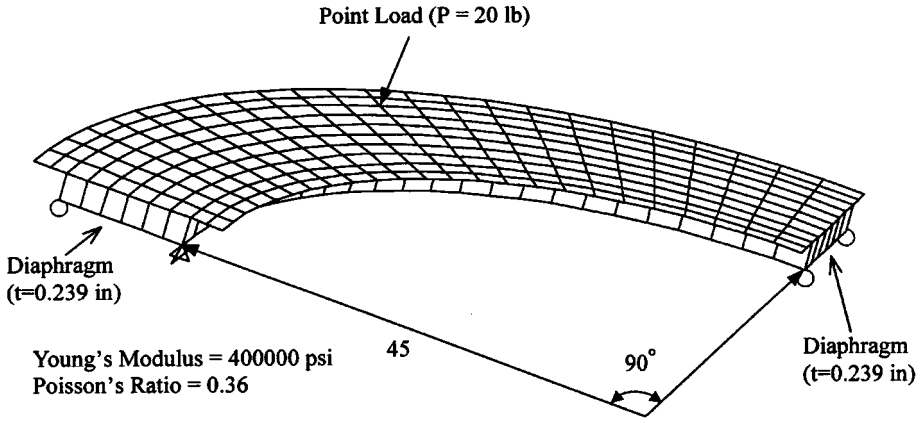

Fig. 20 Curved box girder

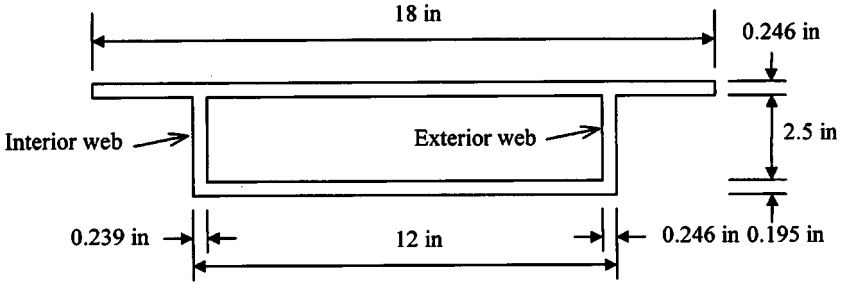

Fig. 21 Section of curved box girder

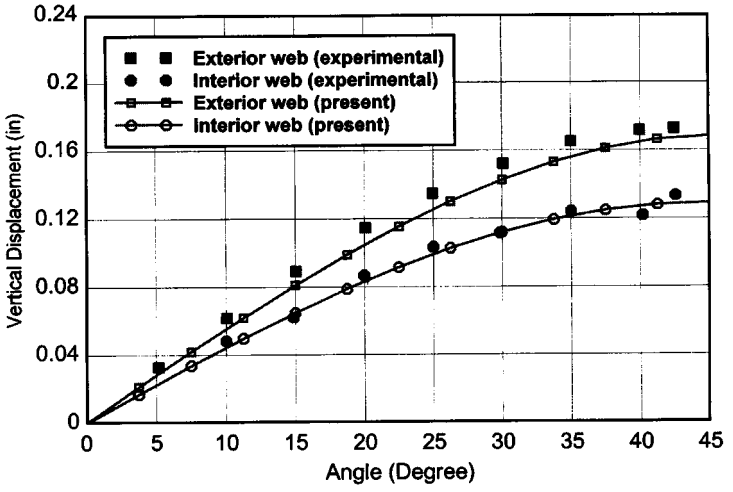

Fig. 22 The vertical displacement of web

series flat shell elements and provides the basis for the development of some variable node elements to follow in the future, such as NMS-5F, NMS-6F, etc.

References

Ahmad, S., Irons, B.M. and Zienkiewicz, O.C. (1968), "Analysis of thick and thin shell structures by curved finite elements", *Int. J. Numer. Methods Eng.*, **2**, 419-451.

Allman, D.J.(1984), "A compatible triangular element including vertex rotation for plane elasticity problems", *Comp. Struct.*, **19**, 1-8 .

Allman, D.J.(1988), "A quadrilateral finite element including vertex rotations for plane elasticity analysis", *Int. J. Numer. Methods Eng.*, **26**, 717-730.

Bergan, P.G. and Felippa., C.A.(1985), "A triangular membrane element with rotational degrees of freedom", *Comp. Methods Appl. Mech. Eng.*, **50**, 25-69.

Choi, C.K. and Schnobrich, W.C.(1975), "Nonconforming finite element analysis of shells", *J. Eng. Mech. Div. ASCE*, **101**, 447-464.

Choi, C.K.(1984), "A conoidal shell analysis by modified isoparametric element", *Comp. Struct.*, **18**, 921-924.

Choi, C.K.(1986), "Reduced integrated nonconforming plate element", *J. Eng. Mech. Div. ASCE*, **112**, 370-385.

Choi, C.K. and Kim, S.H.(1991), "Coupled use of reduced integration and nonconforming modes in quadratic Mindlin plate element", *Comp. Struct.*, **39**, 557-569.

Choi, C.K. and Lee, W.H.(1996), "Versatile variable-node flat shell element", *J. of Eng. Mech. ASCE*, **122**, 432-441.

Choi, C.K., Kim, S.H., Park, Y.M. and Chung, K.Y.(1998), "Two-dimensional nonconforming finite elements: A state-of-art", *Struct. Eng. and Mech.*, **6**(1), 41-61.

Choi, C.K., and Paik, J.G.(1994), "An efficient four node degenerated shell element based on the assumed covariant strain", *Struct. Eng. and Mech.*, **2**(1), 17-34.

Chroscielewski, J., Makowski, J., Stumpf H.(1997), "Finite element analysis of smooth, folded and multi-shell structures", *Comput. Methods Appl. Mech. Eng.* **141**, 1-46.

Cook, R.D.(1986), "On the Allman triangle and a related quadrilateral element", *Comp. Struct.*, **22**, 1065-1067.

Cook, R.D.(1994), "Four-node 'flat' shell element: drilling degrees of freedom, membrane-bending coupling, warped geometry, and behavior", *Comp. Struct.*, **50**, 549-555.

Donea, J. and Lamain, G.(1987), "A modified representation of transverse shear in C^0 quadrilateral plate element", *Comp. Methods Appl. Mech. Eng.*, **63**, 183-207.

Fam, A.R.M. and Turkstra, C.(1976), "Model study of horizontally curved box girder", *J. Eng. Struct. Div. ASCE*, **102**, ST5, 1097-1108.

Frey, F.(1989), "Shell finite elements with six degrees of freedom per node", *Analytical and Computational Models of Shells, CED-Vol.* **3**, ASME, New York.

Gallagher, R.H.(1974), "Finite element representations for thin shell instability analysis", *In Buckling of Structures*, B. Budiansky(ed.), IUTAM Symposiumn, *Cambridge*, MA, 40-51.

Groenwold, A.A. and Stander, N.(1995), "An efficient 4-node 24 D.O.F. thick shell finite element with 5-point quadrature", *Eng. Compu.*, **12**, 723-747.

Hinton, E. and Huang, H.C.(1986), "A family of quadrilateral mindlin plate elements with substitute shear strain fields", *Comp. Struct.*, **23**(3), 409-431.

Hughes, T.J.R., Cohen, M. and Haroun, M.(1978), "Reduced and selective integration techniques in the finite element analysis of plates", *Nuclear Eng. Desg.*, **46**, 203-222.

Hughes, T.J.R. and Brezzi, F.(1989), "On drilling degrees of freedom", *Comp. Methods Appl. Mech. Eng.*, **72**, 105-121.

Hughes, T.J.R. and Tezduyar, T.E.(1981), "Finite elements based upon Mindlin plate theory with

particular reference to the four-node bilinear isoparametric element", *J. of Appl. Mech.*, **48**, 587-596.
Ibrahimbegovic, A. and Frey, F.(1994), "Stress resultant geometrically non-linear shell theory with drilling rotations. Part III: Linearized kinematics", *Int. J. Numer. Methods Eng.*, **37**, 3659-3683.
Ibrahimbegovic, A., Taylor, R.L. and Wilson, E.L.(1990), "A robust quadrilateral membrane finite element with drilling degrees of freedom", *Int. J. Numer. Methods Eng.*, **30**, 445-457.
Iura, M. and Atluri, S.N.(1992), "Formulation of a membrane finite element with drilling degrees of freedom", *Comput. Mech.*, **9**, 417-428.
Jaamei, S., Frey, F. and Jetteur, Ph.(1989), "Nonlinear thin shell finite element with six degrees of freedom per node", *Comp. Methods in Applied Mech. Eng.*, **75**, 251-266.
Jetteur, Ph.(1986), "A shallow shell element with in-plane rotational degrees of freedom", IREM Internal Report 86/3, Ecole Polytechnique Federale de Lausanne.
Jetteur, Ph. and Frey, F.(1986), "A four-node marguerre element for non-linear shell analysis", *Eng. Comput.*, **3**, 276-282.
Kebari, H. and Cassell, A.C.(1991), "Non-conforming modes stabilization of a nine-node stress-resultant degenerated shell element with drilling freedom", *Comp. Struct.*, **40**, 569-580.
Kim, S. H. and Choi, C. K.(1992), "Improvement of quadratic finite element for Mindlin plate bending", *Int. J. Numer. Methods Eng.*, **34**, 197-208.
Lee, S.W. and Wong, S.C.(1982), "Mixed formulation finite elements for Mindlin theory plate bending", *Int. J. Numer. Methods Eng.*, **18**, 1297-1311.
MacNeal, R.H. and Harder, R.L. (1985), "A proposed standard set of problems to test finite element accuracy", *Finite Elements in Anal. Desg.*, **1**, 3-20.
MacNeal, R.H. and Harder, R.L.(1988), "A refined four-noded membrane element with rotational degrees of freedom", *Comp. Struct.*, **28**, 75-84.
Parisch, H.(1979), "A critical survey of the 9-node degenerated shell element with special emphasis on thin shell application and reduced integration", *Comp. Methods Appl. Mech. Eng.*, **20**, 323-350.
Reissner, E.(1965), "A note on variational principles in elasticity", *Int. J. Solids Struct.*, **1**, 93-95.
Sabir, A.B.(1985), "A rectangular and a triangular plane elasticity element with drilling degree of freedom", *Proceedings of the Second International Conference on Variational Methods in Engineering*, Brebbia C.A. (ed.), Southampton University, July 1985, Springer-Verlag, Berlin, 17-55.
SAP 90(1992), Structural Analysis Verification Manual, Computer & Structures Inc.
Simo, J.C., Fox, D.D. and Rifai, M.S.(1989), "On a stress resultant geometrically exact shell model. Part II: The linear theory; Computational aspects", *Comp. Methods Appl. Mech. Eng.*, **73**, 53-92.
Taylor, R.L.(1987), "Finite element analysis of linear shell problems", *Proc. Of the Mathematics in Finite Elements and Applications*, Whiteman, J.R.(ed.), Academic Press, New York, 191-203.
Taylor, R.L. and Simo, J.C.(1985), "Bending and membrane element for analysis of thick and thin shells", *Proceedings of the NUMETA 85 Conference*, Middleton J. and Pande G.N. (eds.), Balkeman Rotterdam, 587-591.
Wilson, E.L. and Ibrahimbegovic, A.(1990), "Use of incompatible displacement modes for the calculation of element stiffnesses or stresses", *Finite Elements in Anal. Desg.*, **7**, 229-241.
Zienkiewicz, O.C. and Taylor, R.L.(1989), *The Finite Element Method: Basic Formulation and Linear Problems*, **I**, McGraw-Hill, London.
Zienkiewicz, O.C., Taylor, R.L. and Too, J.M.(1971), "Reduced integration technique in general analysis of plates and shells", *Int. J. Numer. Methods Eng.*, **3**, 275-290.